TABLE VI: Rate Constants for the Reactions of Doubly and Singly Charged Zr and Ta with Methane

$M^{n+} + CH_4 \rightarrow$ products (n = 1, 2)

	k_{exp}[a]	k_L	k_{exp}/k_L
Zr^+	$(7.1 \pm 4) \times 10^{-12}$	1.03×10^{-9}	0.01
Zr^{2+}	$(5.0 \pm 4) \times 10^{-11}$	2.05×10^{-9}	0.02
Ta^+	$(4.4 \pm 2) \times 10^{-10}$	9.84×10^{-10}	0.45
Ta^{2+}	$(1.95 \pm 1) \times 10^{-9}$	1.97×10^{-9}	1.00

[a] Values are the average and precision of three trials each.

crossings are most favored.[16] One consequence of this reaction window is that charge transfer will not be observed unless the reaction is sufficiently exothermic (≳1 eV). Otherwise, the curve crossing distance is too long to permit electron transfer. For example, the reaction $Zr^{2+} + CH_4 \rightarrow Zr^+ + CH_4^+$ is 0.6 eV exothermic but is not observed due to a curve crossing distance of about 23 Å (Table V). Similarly, Ar^+ is not produced during the cooling period for Ta^{2+} even though the reaction is about 0.44 eV exothermic. In addition, the product branching ratios for Zr^{2+}, and in our earlier study for Nb^{2+}, can also be explained in terms of this reaction window. Weisshaar et al.[5a] observed mainly the adduct ion in the reaction of Ti^{2+} with CH_4 and hydride transfer almost exclusively with C_2H_6. Bond insertion and hydride transfer occur in the reactions of Zr^{2+} with both methane and ethane. For both Ti^{2+} and Zr^{2+} hydride abstraction is a major pathway with ethane. Bond insertion reactions and hydride transfer compete effectively with charge transfer in the reactions of Zr^{2+} with C_3H_8, while for Ti^{2+} only hydride and charge transfer were observed. The percentage of charge transfer rises sharply for C_4H_{10} and the higher alkanes in accord with the relevant curve crossings lying within the reaction window. The general tendency for production of the charge-separated product in the CID of $TaC_2H_2^{2+}$, reaction 14, and the enhanced production of Zr^{2+} in the CID of the analogous zirconium species, reaction 30, are also in accord with the curve-crossing model.

For Nb^{2+}, ≥99% charge transfer was observed with C_3H_8 having an estimated curve crossing at 4.8 Å, while for Zr^{2+} this occurred for n-C_5H_{12} with a curve crossing at 5.7 Å. Considering that the curve crossing for Ta^{2+} and CH_4 is 4.2 Å, it is somewhat surprising, therefore, that charge transfer is not the predominant reaction observed. This "discrepancy" underlines the fact that this model is after all an oversimplification. The limitations of this model and the associated Landau-Zener[17] approach to calculating curve-crossing probabilities and charge-transfer cross sections have been discussed by a number of researchers.[4a,18] In the present study, several factors can limit the applicability of this approach, including the multiplicity of curve crossings and the possibility of extensive state coupling given the high density of states of the M^{2+} species. Furthermore, the surfaces do not include details of the impact parameter and collision geometry. A variety of other limitations have been previously discussed. Nevertheless, while clearly not rigorous, this and previous studies suggest that the model does provide a useful qualitative picture.

Acknowledgment is made to the Division of Chemical Sciences in the Office of Basic Energy Sciences in the United States Department of Energy (DE-FG02-87ER13766) for supporting this research and to the National Science Foundation (CHE-8920085) for continued support of FTMS methodology.

Registry No. Ta^{2+}, 35831-23-3; Zr^{2+}, 14995-75-6; Zr^+, 14701-19-0; CH_4, 74-82-8; EtH, 74-84-0; PrH, 74-98-6; BuH, 106-97-8; $H_3C(CH_2)_3CH_3$, 109-66-0.

(16) Smith, D.; Adams, N. G.; Alge, E.; Villinger, H.; Lindinger, W. *J. Phys.* **1980**, *B13*, 2787.

(17) (a) Landau, L. *Z. Phys. Sowjet* **1932**, *2*, 46. (b) Zener, C. *Proc. R. Soc. London, Ser. A* **1932**, *137*, 696.

(18) (a) Bates, D. R.; Moiseiwitsch, B. L. *Proc. Phys. Soc., London* **1954**, *A67*, 805. (b) Hasted, J. B.; Chong, A. Y. *Proc. Phys. Soc., London* **1962**, *A80*, 441.

Kinetics of the Reactions of CS_2OH with O_2, NO, and NO_2

Eric Wei-Guang Diau and Yuan-Pern Lee*,†

Department of Chemistry, National Tsing Hua University, 101, Sec. 2, Kuang Fu Road, Hsinchu, Taiwan 30043, Republic of China *(Received: January 29, 1991)*

The laser-photolysis/laser-induced-fluorescence technique has been employed to study the reactions of CS_2OH with O_2, NO, and NO_2 in the presence of He at 26-202 Torr and 298 K. With excess CS_2 and without O_2, NO, and NO_2, a rapid approach of [OH] to equilibrium was observed, indicating reversible formation of a CS_2OH adduct. When O_2, NO, or NO_2 was present at a small concentration, a rapid decrease of [OH] after reaching equilibrium was observed. Analysis of the [OH] temporal profiles yielded the rate coefficients for each reaction. The coefficients are $k(CS_2OH+O_2) = (3.1 \pm 0.6) \times 10^{-14}$, $k(CS_2OH+NO) = (7.3 \pm 1.8) \times 10^{-13}$, and $k(CS_2OH+NO_2) = (4.2 \pm 1.0) \times 10^{-11}$ cm^3 molecule^{-1} s^{-1}; the uncertainties represent 95% confidence limits.

Introduction

The oxidation of CS_2 is important in the atmosphere and has been the subject of many investigations. The reaction of CS_2 with OH has been generally accepted to be the major pathway for the degradation of CS_2 to form OCS and SO_2.[1] Previous laboratory studies of this reaction have reported rate coefficients that varied by 2 orders of magnitude.[2-9] A rate enhancement in the presence of O_2 has also been reported.[10-15] The reaction mechanism

$$OH + CS_2 \xrightarrow{M} CS_2OH \quad (1f)$$

$$CS_2OH \xrightarrow{M} OH + CS_2 \quad (1r)$$

$$CS_2OH + O_2 \rightarrow \text{products} \quad (2)$$

has been employed to explain the observed experimental results. With excess CS_2 and without O_2, a rapid approach of [OH] to

† Also affiliated with the Institute of Atomic and Molecular Sciences, Academia Sinica, Taiwan, Republic of China.

(1) Finlayson-Pitts, B. J.; Pitts, J. N., Jr. *Atmospheric Chemistry*; Wiley: New York, 1986; p 663.

0022-3654/91/2095-7726$02.50/0

equilibrium within 10^{-5} s has been recently observed by means of the pulsed laser-photolysis/laser-induced-fluorescence technique.[13-17] Analysis of the [OH] temporal profiles yielded the rate coefficients for k_{1f} and k_{1r}, and hence, the equilibrium constant for reaction 1.

When O_2 was present, an enhancement of the OH loss rate in CS_2 was observed, indicating the occurrence of reaction 2. Hynes et al. investigated reaction 2 under atmospheric conditions and reported a temperature-independent value $k_2 = (2.9 \pm 1.1) \times 10^{-14}$ cm^3 $molecule^{-1}$ s^{-1} by using a steady-state approximation based on the above three-step mechanism.[13] Murrells et al. recently studied reaction 2 with $O_2 < 8$ Torr in He at 50 Torr; they analyzed the [OH] temporal profile and obtained a temperature-independent value $k_2 = (2.6 \pm 1.0) \times 10^{-14}$ cm^3 $molecule^{-1}$ s^{-1} for $T = 249$–299 K.[14]

Similarly, in the presence of NO, rapid loss of OH in CS_2 due to the reaction

$$CS_2OH + NO \rightarrow \text{products} \quad (3)$$

has also been observed by Lovejoy et al.; $k_3 = (1.3 \pm 0.4) \times 10^{-12}$ and $(9.1 \pm 3.5) \times 10^{-13}$ cm^3 $molecule^{-1}$ s^{-1} at 249 and 299 K, respectively, were reported.[18] Using a similar technique, Bulatov et al. also investigated the reaction

$$CS_2OH + O_3 \rightarrow \text{products} \quad (4)$$

and reported $k_4 = (9 \pm 3) \times 10^{-13}$ cm^3 $molecule^{-1}$ s^{-1} at 298 K.[16]

The reactions of the CS_2OH adduct with these molecules appeared to be relatively rapid. It is therefore interesting to explore other possible reactions of CS_2OH which may be important in related kinetics studies. We have determined the rate coefficients for the reactions of CS_2OH with O_2, NO, and NO_2 by means of the laser-photolysis/laser-induced-fluorescence technique. The reaction of CS_2OH with NO_2 showed a relatively large rate coefficient; hence the reaction is likely to have interfered with previous measurements in which NO_2 was present.

Experimental Section

The laser-photolysis/laser-induced-fluorescence technique and the experimental setup have been described in detail previously;[17] hence only a summary is given here.

The OH radicals were generated by laser photolysis of H_2O_2 or HNO_3 at 248 nm and, after a certain delay, were excited at 282 nm to the $\tilde{A}$ state; the laser-induced fluorescence of OH was detected near 309 nm. The temporal profile of the OH concentration was obtained by combining 3–5 sets of data each of which consisted of [OH] measurements at 20 evenly spaced time intervals after photolysis; the maximum delay in each set was in the range 0.1–20 ms. For each measurement of [OH], the fluorescence signal was averaged over 120 pulses at 10 Hz repetition rate.

Typical experimental conditions were as follows: total flow rate $F_T = 2$–14 STP cm^3 s^{-1}; $P = 26$–202 Torr; $T = 298$ K; $[CS_2] = (3.5$–$6.3) \times 10^{16}$ molecules cm^{-3}; $[OH]_0 \simeq (0.8$–$5.0) \times 10^{11}$ molecules cm^{-3}; $[HNO_3] \simeq (4$–$20) \times 10^{14}$ molecules cm^{-3} or $[H_2O_2] \simeq (4$–$8) \times 10^{13}$ molecules cm^{-3}.

The diluent gas He (99.9995%) was used without further purification. CS_2 (99.9%) was purified by vacuum distillation between 77 and 210 K. H_2O_2 (~90%) was concentrated by bubbling He or Ar through a 70% aqueous solution for several days. HNO_3 was prepared by the reaction of $NaNO_3$ with H_2SO_4 (95–97%), followed by vacuum distillation between 77 and 298 K. NO_2 was prepared by slow reaction of NO with O_2 and was stored under O_2 at a few times atmospheric pressure before use. A mixture of NO_2 (0.76%) in He was used in the experiments because only minute concentrations of NO_2 were needed due to its rapid reactions. The concentration of the mixture was calibrated by infrared spectrometry. NO (99%) was purified by vacuum distillation between 77 and 163 K to remove impurities such as NO_2. The purities of NO and NO_2 were also checked by means of the infrared spectrometry.

Results and Discussion

The reactions were studied under experimental conditions such that $[CS_2] \gg [OH]_0$, similar to those in our previous study[17] of reaction 1 except that a small amount of O_2, NO, or NO_2 was added into the system. In our previous study of the equilibrium reaction of $OH + CS_2 + M \rightleftharpoons CS_2OH + M$, the [OH] temporal profiles were characterized by an initial rapid decay followed by a much slower decay toward the millisecond range of reaction time. In this study, $[O_2]$ (or [NO], $[NO_2]$) was normally kept small so as not to perturb greatly the equilibrium between reactions 1f and 1r; hence the double-exponential decay of OH was still observable. Appropriate $[CS_2]$ was also chosen to assure that $[OH]_{eq}$, the equilibrium concentration of OH in the absence of the reactants O_2, NO, and NO_2, was in the range $(0.4$–$0.8)[OH]_0$.

A simple mechanism which consists the following reactions

$$OH + CS_2 \xrightarrow{M} CS_2OH \quad (1f)$$

$$CS_2OH \xrightarrow{M} OH + CS_2 \quad (1r)$$

$$CS_2OH \rightarrow \text{products other than OH} \quad (5)$$

$$OH \rightarrow \text{products other than } HOCS_2 \quad (6)$$

was used to model the temporal profile of [OH]. In the absence of reactants other than OH and CS_2, the diffusion of CS_2OH from the probed volume mainly accounted for reaction 5; k_5 was typically in the range 50–150 s^{-1}. In the presence of O_2, reaction 2 became the major path for the loss of CS_2OH. Similarly, reactions 3 and 7

$$CS_2OH + NO \rightarrow \text{products} \quad (3)$$

$$CS_2OH + NO_2 \rightarrow \text{products} \quad (7)$$

were the major paths for the loss of CS_2OH, respectively, when NO and NO_2 were present. The value of k_6 also increased when NO or NO_2 was present; this effect is discussed hereafter.

As described previously,[17] the four-step mechanism yields a double-exponential [OH] decay profile provided that $[CS_2] \gg [OH]_0$:

$$[OH] = [OH]_0[(\gamma + \lambda_1)\exp(\lambda_1 t) - (\gamma + \lambda_2)\exp(\lambda_2 t)]/(\lambda_1 - \lambda_2) \quad (8)$$

in which

$$\lambda_1 = [(\alpha^2 - 4\beta)^{1/2} - \alpha]/2 < 0 \quad (9)$$

$$\lambda_2 = -[(\alpha^2 - 4\beta)^{1/2} + \alpha]/2 < 0 \quad (10)$$

$$\gamma = k_{1r} + k_5 \quad (11)$$

$$\alpha = k_{1f}[CS_2] + k_{1r} + k_5 + k_6 \quad (12)$$

$$\beta = k_{1f}k_5[CS_2] + k_{1r}k_6 + k_5k_6 \quad (13)$$

k_{1f} and k_{1r} are the apparent second-order and first-order rate

(2) Kurylo, M. J. *Chem. Phys. Lett.* **1978**, *58*, 238.
(3) Kurylo, M. J.; Laufer, A. H. *J. Chem. Phys.* **1979**, *70*, 2032.
(4) Cox, R. A.; Sheppard, D. *Nature* **1980**, *284*, 330.
(5) Atkinson, R.; Perry, R. A.; Pitts, J. N., Jr. *Chem. Phys. Lett.* **1978**, *54*, 14.
(6) Wine, P. H.; Shah, R. C.; Ravishankara, A. R. *J. Phys. Chem.* **1980**, *84*, 2499.
(7) Leu, M. T.; Smith, R. H. *J. Phys. Chem.* **1982**, *86*, 958.
(8) Biermann, H. W.; Harris, G. W.; Pitts, J. N., Jr. *J. Phys. Chem.* **1982**, *86*, 2958.
(9) Iyer, R. S.; Rowland, F. S. *Geophys. Res. Lett.* **1980**, *7*, 797.
(10) Jones, B. M. R.; Burrows, J. P.; Penkett, S. A. *Chem. Phys. Lett.* **1982**, *88*, 372.
(11) Jones, B. M. R.; Cox, R. A.; Penkett, S. A. *J. Atmos. Chem.* **1983**, *1*, 65.
(12) Barnes, I.; Becker, K. H.; Fink, E. H.; Reimer, A.; Zabel, F.; Niki, H. *Int. J. Chem. Kinet.* **1983**, *15*, 631.
(13) Hynes, A. J.; Wine, P. H.; Nicovich, J. M. *J. Phys. Chem.* **1988**, *92*, 3846.
(14) Murrells, T. P.; Lovejoy, E. R.; Ravishankara, A. R. *J. Phys. Chem.* **1990**, *94*, 2381.
(15) Becker, K. H.; Nelsen, W.; Su, Y.; Wirtz, K. *Chem. Phys. Lett.* **1990**, *168*, 559.
(16) Bulatov, V. P.; Cheskis, S. G.; Iogansen, A. A.; Kulakov, P. V.; Sarkisov, O. M.; Hassinen, E. *Chem. Phys. Lett.* **1988**, *153*, 258.
(17) Diau, Eric W.-G.; Lee, Y.-P. *J. Phys. Chem.* **1991**, *95*, 379.
(18) Lovejoy, E. R.; Murrells, T. P.; Ravishankara, A. R.; Howard, C. J. *J. Phys. Chem.* **1990**, *94*, 2386.

TABLE I: Summary of Experimental Conditions, Decay Parameters of the [OH] Temporal Profile, and the Rate Coefficients for the Study of the Reaction $CS_2OH + O_2 \rightarrow$ Products in Helium at 298 K[a]

expt no.	P/Torr	$[CS_2]/10^{16}$ [b]	$[O_2]/10^{16}$ [b]	$\alpha/10^4$ s^{-1}	$\beta/10^7$ s^{-2}	$\gamma/10^4$ s^{-1}	k_6/s^{-1}	$k_5/10^3$ s^{-1}
1	65	4.37	11.2	3.21 ± 0.24	3.86 ± 0.31	2.23 ± 0.18	83.7 ± 1.9	3.77 ± 1.24
2		4.24	5.01	3.17 ± 0.13	2.01 ± 0.09	2.18 ± 0.10		1.87 ± 0.35
3		4.16	1.63	3.01 ± 0.12	0.89 ± 0.04	2.14 ± 0.09		0.82 ± 0.16
4		4.43	15.3	3.71 ± 0.29	5.92 ± 0.49	2.66 ± 0.23		5.46 ± 2.02
5		4.58	23.8	3.46 ± 0.25	7.54 ± 0.60	2.47 ± 0.21		7.52 ± 2.65
6		4.29	8.09	3.41 ± 0.16	3.03 ± 0.15	2.49 ± 0.13		3.07 ± 0.74
7		4.49	18.6	3.39 ± 0.17	5.97 ± 0.32	2.49 ± 0.14		6.41 ± 1.68
8		4.16	3.28	3.26 ± 0.14	1.47 ± 0.06	2.45 ± 0.11		1.59 ± 0.37
9		4.56	26.1	4.10 ± 0.19	9.55 ± 0.47	2.99 ± 0.16		8.45 ± 2.01
10		4.33	13.5	3.62 ± 0.22	4.84 ± 0.30	2.71 ± 0.18		5.15 ± 1.67
11	100	6.26	14.3	5.47 ± 0.22	9.43 ± 0.41	3.57 ± 0.16	78.2 ± 2.5	4.83 ± 0.80
12		5.84	6.33	4.59 ± 0.21	4.03 ± 0.20	2.87 ± 0.14		2.22 ± 0.38
13		6.00	22.3	5.68 ± 0.27	15.36 ± 0.81	3.60 ± 0.20		7.25 ± 1.34
14		5.70	10.5	4.66 ± 0.17	6.16 ± 0.24	3.00 ± 0.12		3.60 ± 0.54
15		5.90	28.7	5.25 ± 0.20	16.44 ± 0.72	3.36 ± 0.16		8.60 ± 0.54
16		5.91	32.5	6.60 ± 0.43	25.37 ± 1.82	4.37 ± 0.33		11.29 ± 2.98
17	140	5.76	18.5	5.62 ± 0.32	11.84 ± 0.73	3.67 ± 0.23	92.1 ± 5.6	5.94 ± 1.34
18		5.42	5.32	4.98 ± 0.25	3.51 ± 0.19	3.26 ± 0.18		1.87 ± 0.38
19		5.41	12.3	6.14 ± 0.34	8.66 ± 0.52	4.04 ± 0.24		3.96 ± 0.88

[a] The uncertainties represent 1 standard deviation. [b] In units of molecules cm^{-3}.

coefficients for reactions 1f and 1r, respectively; k_5 and k_6 are the apparent first-order rate coefficients for reactions 5 and 6, respectively. The observed temporal profiles of [OH] were fitted to eq 8 by using a nonlinear least-squares method to determine λ_1, λ_2, and γ. Because reactions 2, 3, and 7 greatly enhanced the loss rate of CS_2OH, the accuracies of k_{1f} and k_{1r} were not as good as those reported previously[17] when no oxidant was present in the system. However, the accuracy of k_5 (which gave k_2, k_3, or k_7) was reasonably good when the concentration of the oxidants were properly chosen. Rearrangement of eqs 11–13 gives

$$k_5 = (\beta - k_6\gamma)/(\alpha - \gamma - k_6) \quad (14)$$

The values of k_6 were determined experimentally from the single-exponential OH decay under similar conditions except that $[CS_2] = 0$.

1. The $CS_2OH + O_2$ Reaction. The rate of the slower component of the OH decay in the OH + CS_2 system increased when O_2 was added into the system. Figure 1 shows typical temporal profiles of [OH] with and without O_2 added to He at ~65 Torr and 298 K. The enhancement of the OH loss due to the presence of O_2 is clearly illustrated.

The loss of OH other than reaction 1f (i.e., reaction 6 in the four-step mechanism) is mainly due to the reaction

$$OH + H_2O_2 \rightarrow HO_2 + H_2O \quad (15)$$

in which $k_{15} = 1.7 \times 10^{-12}$ cm^3 molecule^{-1} s^{-1}.[19] The value of k_6, determined with no CS_2 in the system, was kept less than 100 s^{-1} by using small concentrations of H_2O_2 and OH. The experimental conditions, the decay parameters α, β, and γ (derived by fitting the OH temporal profile to eq 8), and the rate coefficients k_6 and k_5 are listed in Table I. The values of k_5 were derived from eq 14.

The bimolecular rate coefficient for reaction 2, k_2, is related to k_5 by the equation

$$k_5 = k_2[O_2] + k' \quad (16)$$

in which k' refers to all loss processes for CS_2OH other than reactions 1r and 2. Figure 2 shows a plot of k_5 versus $[O_2]$ under a total pressure of 65–140 Torr at 298 K. The partial pressure of O_2 was in the range 0.5–10 Torr. A least-squares fit of k_5 to eq 16 gave $k_2 = (3.12 \pm 0.07) \times 10^{-14}$ cm^3 molecule^{-1} s^{-1} at 298 K. The uncertainties listed in this paper represent 1 standard deviation unless otherwise stated. The data showed no pressure dependence in the range of study, indicating the bimolecular nature of reaction 2. The systematic errors in these experiments are estimated to be less than ±15%;[17] hence we report $k_2 = (3.1 \pm 0.6) \times 10^{-14}$ cm^3 molecule^{-1} s^{-1} with the uncertainties representing 95% confidence limits. The intercept in Figure 2, $k' = 380 \pm 60$

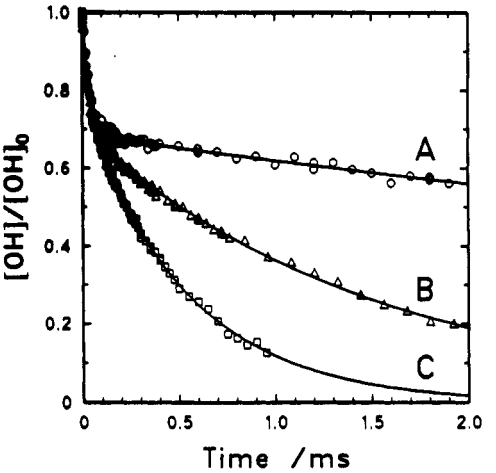

Figure 1. Temporal profiles of [OH] in the presence of CS_2 at various concentrations of O_2. $[O_2]/10^{16}$ molecules cm^{-3} = 0 (A); 5.0 (B); 18.6 (C). T = 298 K, P = 65 Torr (He), $[OH]_0 \simeq 1 \times 10^{11}$ molecules cm^{-3}, $[H_2O_2] \simeq 5 \times 10^{13}$ molecules cm^{-3}, $[CS_2] = 4.2 \times 10^{16}$ (for A and B) and 4.5×10^{16} (for C) molecules cm^{-3}. The solid lines are obtained from the nonlinear least-squares fit described in the text.

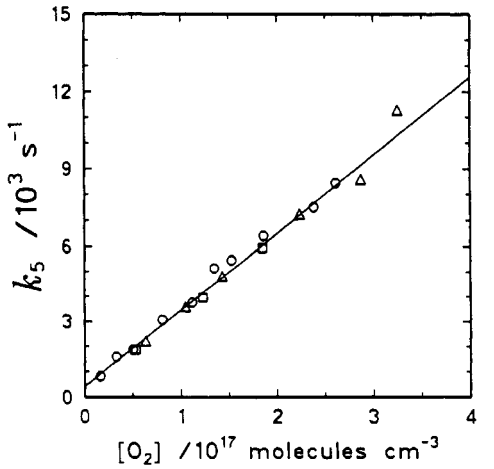

Figure 2. First-order rate coefficient of CS_2OH loss (other than reaction 1r), k_5, as a function of O_2 concentration at 298 K. $[H_2O_2] \simeq$ (4–6) × 10^{13} molecules cm^{-3}; (○) P = 65 Torr, $[OH]_0 \simeq 1 \times 10^{11}$ molecules cm^{-3}; (△) P = 100 Torr, $[OH]_0 \simeq 0.9 \times 10^{11}$ molecules cm^{-3}; (□) P = 140 Torr, $[OH]_0 \simeq 2 \times 10^{11}$ molecules cm^{-3}.

(19) Keyser, L. F. *J. Phys. Chem.* **1980**, *84*, 1659.

s^{-1}, is slightly greater than, but comparable to, the k_5 values (50–250 s^{-1}, listed as k_3 in ref 17) observed in our previous studies of reaction 1 in the absence of O_2. The equilibrium constant, $K_c = k_{1f}/k_{1r}$, could also be determined by solving k_{1f} and k_{1r} from eqs 11–13 with given values of k_6. The results $K_c = (1.09 \pm 0.21) \times 10^{-17}$ cm^3 $molecule^{-1}$, although less accurate due to effects from the large values of k_6, are in reasonable agreement with the value $K_c = (0.87 \pm 0.17) \times 10^{-17}$ cm^3 $molecule^{-1}$ determined previously in the absence of O_2.[17]

Our value $k_2 = (3.1 \pm 0.6) \times 10^{-14}$ cm^3 $molecule^{-1}$ s^{-1} is slightly greater than the value $(2.6 \pm 1.0) \times 10^{-14}$ cm^3 $molecule^{-1}$ s^{-1} reported recently by Murrells et al.;[14] the uncertainties overlap in the two studies. The experimental conditions were similar in both studies. Murrells obtained values of k_5 by fitting the [OH] temporal profiles to eq 8 with k_{1f}, k_{1r}, and k_6 fixed at values derived from experiments without O_2. We also analyzed our data by using this method and obtained a similar but slightly more scattered data set. Presumably this was because k_{1f} and k_{1r} are dependent on the identity and the concentration of the third body, as reported in our previous study;[17] the third-body effect for $M = O_2$ could not be accurately evaluated. In both studies, O_2 at less than 10 Torr was added to the system so that the initial rapid approach of OH to equilibrium could be separated from the subsequent slower decay of OH due to mostly reaction 2. In comparison, most data of the study of reaction 2 by Hynes et al. were determined with $P_{O_2} \simeq 140$ Torr.[13] Single-exponential decays of OH were observed under such conditions and the k_2 values were obtained from a complex data analysis on the basis of a steady-state approximation of CS_2OH. It is surprising that the average value of k_2 (listed as k_3 in ref 13) reported by Hynes et al. $(2.9 \pm 1.1) \times 10^{-14}$ cm^3 $molecule^{-1}$ s^{-1}, is almost identical with our value, in view of the relatively large uncertainties involved in their analysis.

If a reaction mechanism consisting of reactions 1f, 1r, and 2 is used in the steady-state approximation of CS_2OH, the observed effective rate coefficient for OH decay, k_{obsd}, may be expressed as

$$k_{obsd} \simeq k_2[O_2]K_c \qquad (17)$$

in which K_c is the equilibrium constant for reaction 1. With $K_c = 8.7 \times 10^{-18}$ cm^3 $molecule^{-1}$ determined previously and $k_2 = (3.1 \pm 0.6) \times 10^{-14}$ cm^3 $molecule^{-1}$ s^{-1}, k_{obsd} was estimated to be approximately 1.3×10^{-12} cm^3 $molecule^{-1}$ s^{-1} under atmospheric conditions at 298 K. The value is slightly smaller than, but within experimental uncertainties of, the values $(1.5 \pm 0.1) \times 10^{-12}$ cm^3 $molecule^{-1}$ s^{-1} reported by Hynes et al.[13] and $(1.7 \pm 0.9) \times 10^{-12}$ cm^3 $molecule^{-1}$ s^{-1} reported by Jones et al. who photolyzed $CS_2/HONO/O_2/N_2$ mixtures and monitored the formation of OCS and SO_2 by means of gas chromatography.[10,11] However, Barnes et al. have photolyzed $CH_3ONO/N_2/O_2/C_4H_{10}$ mixtures and monitored CS_2, OCS, and SO_2 by infrared spectrometry, and C_4H_{10} by gas chromatography; a value $k_{obsd} = (2.7 \pm 0.6) \times 10^{-12}$ cm^3 $molecule^{-1}$ s^{-1} at 293 K was derived by comparison of the observed rate with that of the reaction $OH + C_4H_{10}$.[12] Recent study by Becker et al.[15] using similar techniques supported the value reported by Barnes et al. A mechanism consisting of the formation of an intermediate in reaction 2 which subsequently decomposed to regenerate OH or reacted with a second O_2 molecule to form HO_2, COS, and SO_2 was proposed to account for the difference between the rate coefficient k_{obsd} determined by the absolute measurements and those determined by the relative method. However, no definitive support for this mechanism has been reported yet. We did not observe any dependence of k_{1r} on $[O_2]$, indicating that if the proposed mechanism is true, reaction 2 must be much slower than the decomposition of the intermediate formed in reaction 2; reaction 2 is therefore rate-determining.

2. The CS_2OH + NO Reaction. NO is more effective in removing CS_2OH than O_2; hence smaller concentrations of NO, $(0.7–9.2) \times 10^{15}$ cm^3 $molecule^{-1}$, were used. The values of k_6 measured in the OH + NO system are also much greater than those in the OH + O_2 system mainly because NO reacts with OH via the reaction

$$OH + NO + M \rightarrow HONO + M \qquad (18)$$

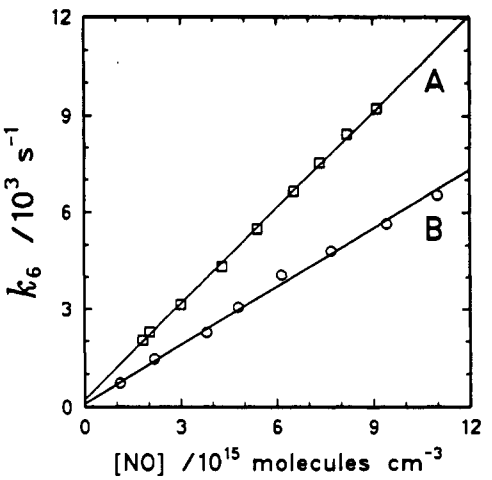

Figure 3. First-order rate coefficient of OH loss (other than reaction 1f), k_6, as a function of NO concentration of 298 K. (A) $P = 122$ Torr, $[HNO_3] \simeq 5 \times 10^{14}$ molecules cm^{-3}, $[OH]_0 \simeq 1 \times 10^{11}$ molecules cm^{-3}; (B) $P = 65$ Torr, $[H_2O_2] \simeq 8 \times 10^{13}$ molecules cm^{-3}, $[OH]_0 \simeq 2 \times 10^{11}$ molecules cm^{-3}.

in which $k_{17}^0 = (4.4 \pm 1.0) \times 10^{-31}$ cm^6 $molecule^{-2}$ s^{-1} for M = He,[20] and $k_{17}^\infty = (1.5 \pm 1.0) \times 10^{-11}$ cm^3 $molecule^{-1}$ s^{-1} at 300 K.[21] A plot of k_6 versus [NO] is shown in Figure 3 for $P = 65$ and 122 Torr. At 298 K, the bimolecular rate coefficient was determined to be $(6.02 \pm 0.15) \times 10^{-13}$ and $(9.86 \pm 0.11) \times 10^{-13}$ cm^3 $molecule^{-1}$ s^{-1} at 65 and 122 Torr (He), respectively, in good agreement with previous measurements.[20,21] When H_2O_2 was used as a source of OH, the intercept in trace B of Figure 3, 95 ± 68 s^{-1}, reflects the contribution of the OH loss due to reaction 15; the values agree with those (k_6 in Table I) observed in the $CS_2OH + O_2$ study and are relatively small compared with the k_6 values in this study. The trace HO_2 produced from reaction 15 was cycled back to OH via the reaction

$$HO_2 + NO \rightarrow OH + NO_2 \qquad (19)$$

in which $k_{19} = 8.3 \times 10^{-12}$ cm^3 $molecules^{-1}$ s^{-1} at 298 K. Although this interference was estimated to be small, HNO_3 was also used as an alternative source of OH in order to minimize the possible error. When HNO_3 was used as a source of OH, the reaction

$$OH + HNO_3 \rightarrow \text{products} \qquad (20)$$

in which $k_{20} \simeq (1.0–1.5) \times 10^{-13}$ cm^3 $molecule^{-1}$ s^{-1} at 298 K depending on pressure,[21] also contributes to the loss of OH. The intercept in trace A of Figure 3 (224 ± 49 s^{-1}), slightly greater than the expected OH loss rate due to reaction 20, is also relatively small compared with the k_6 values determined in this study.

For each experiment k_6 was determined first from the OH + NO system; CS_2 was then added to the system and the double-exponential decay of OH determined. The value of k_5 was then derived from eq 14 with the k_6 value measured from the previous experiments. The experimental conditions, the decay parameters, α, β, and γ, and the rate coefficients k_6 and k_5 are listed in Table II. A plot of k_5 versus [NO] at 298 K and $P = 64$, 65, and 122 Torr is shown in Figure 4. In experiments at $P = 65$ Torr, HNO_3 was replaced by H_2O_2 as a source of OH; no change in k_5 was observed. The rate coefficient k_5 may be expressed as

$$k_5 = k_3[NO] + k'' \qquad (21)$$

(20) The listed coefficient is the average value of four reports: (a) Morley, C.; Smith, I. W. M. *J. Chem. Soc., Faraday Trans. 2* **1972**, *68*, 1016. (b) Howard, C. J.; Evenson, K. M. *J. Chem. Phys.* **1974**, *61*, 1943. (c) Anderson, J. G.; Margitan, J. J.; Kaufman, F. *J. Chem. Phys.* **1974**, *60*, 3310. (d) Burrows, J. P.; Wallington, T. J.; Wayne, R. P. *J. Chem. Soc., Faraday Trans. 2* **1983**, *79*, 111.

(21) DeMore, W. B.; Molina, M. J.; Sander, S. P.; Hampson, R. F.; Kurylo, M. J.; Golden, D. M.; Howard, C. J.; Ravishankara, A. R. "Chemical Kinetics and Photochemical Data for Use in Stratospheric Modeling"; Publication 87-41, Jet Propulsion Laboratory, Pasadena, CA, 1987.

TABLE II: Summary of Experimental Conditions, Decay Parameters of the [OH] Temporal Profile, and the Rate Coefficients for the Study of the Reaction $CS_2OH + NO \rightarrow$ Products in Helium at 298 K[a]

expt no.	P/Torr	$[CS_2]/10^{16}$ [b]	$[NO]/10^{15}$ [b]	$\alpha/10^4$ s^{-1}	$\beta/10^7$ s^{-2}	$\gamma/10^4$ s^{-1}	$k_6/10^3$ s^{-1}	$k_5/10^3$ s^{-1}
1	64	3.76	2.86	3.03 ± 0.13	5.15 ± 0.24	2.01 ± 0.10	1.86 ± 0.06	1.69 ± 0.52
2		3.73	0.70	2.64 ± 0.13	1.47 ± 0.07	1.84 ± 0.10	0.585 ± 0.02	0.527 ● 0.18
3		3.70	8.33	3.01 ± 0.20	13.02 ± 1.20	1.76 ± 0.19	5.09 ± 0.15	5.49 ± 2.99
4		3.65	4.15	2.81 ± 0.14	6.87 ± 0.40	1.80 ± 0.12	2.62 ± 0.08	2.88 ± 1.00
5		3.62	7.12	3.55 ± 0.20	14.52 ± 1.02	2.25 ± 0.18	4.37 ± 0.13	5.42 ± 2.31
6		3.59	2.10	3.22 ± 0.16	4.68 ± 0.26	2.23 ± 0.13	1.41 ± 0.04	1.82 ± 0.61
7		3.56	5.66	3.56 ± 0.24	12.09 ± 0.97	2.33 ± 0.21	3.51 ± 0.11	4.47 ± 2.17
8		3.53	1.51	2.63 ± 0.15	2.70 ± 0.17	1.83 ± 0.12	1.06 ± 0.03	1.09 ± 0.45
9	65	4.79	3.87	3.89 ± 0.13	9.58 ± 0.36	2.59 ± 0.10	2.46 ± 0.07	3.06 ± 0.64
10		4.79	6.92	3.93 ± 0.19	15.51 ± 0.87	2.57 ± 0.16	4.25 ± 0.13	4.85 ± 1.79
11		4.79	1.26	3.99 ± 0.21	3.44 ± 0.19	2.65 ± 0.15	0.92 ± 0.03	0.82 ± 0.27
12		4.79	9.19	3.75 ± 0.23	18.82 ± 1.48	2.32 ± 0.21	5.59 ± 0.17	6.68 ± 3.27
13		4.79	5.22	3.51 ± 0.15	10.87 ± 0.57	2.24 ± 0.13	3.25 ± 0.10	3.82 ± 1.16
14		4.79	8.05	4.10 ± 0.22	19.02 ± 1.27	2.55 ± 0.19	4.92 ± 0.15	6.10 ± 2.32
15	122	4.56	3.17	5.08 ± 0.26	13.98 ± 0.82	3.29 ± 0.20	3.35 ± 0.10	2.04 ± 0.91
16		4.65	1.87	5.42 ± 0.34	10.13 ± 0.69	3.62 ± 0.25	2.06 ± 0.02	1.67 ± 0.72
17		4.74	5.56	4.75 ± 0.31	21.75 ± 1.89	2.72 ± 0.26	5.72 ± 0.17	4.26 ● 2.08
18		4.82	4.26	4.76 ± 0.34	18.03 ± 1.55	2.96 ± 0.28	4.43 ± 0.13	3.63 ± 1.92

[a] The uncertainties represent 1 standard deviation. [b] In units of molecules cm^{-3}.

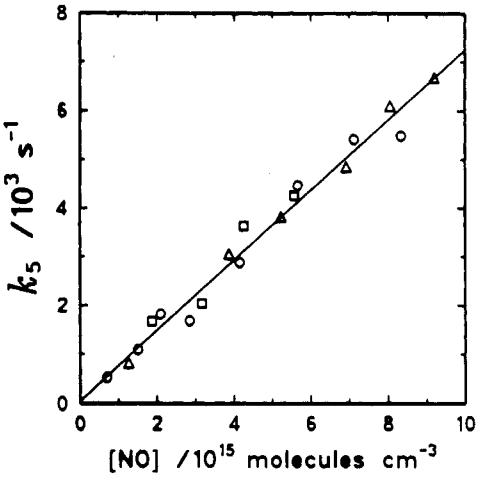

Figure 4. First-order rate coefficient of CS_2OH loss (other than reaction 1r), k_5, as a function of NO concentration at 298 K. (○) P = 64 Torr, $[HNO_3] \simeq 7 \times 10^{14}$ molecules cm^{-3}, $[OH]_0 \simeq (1-2) \times 10^{11}$ molecules cm^{-3}; (△) P = 65 Torr, $[H_2O_2] \simeq 8 \times 10^{13}$ molecules cm^{-3}, $[OH]_0 \simeq (0.9-2) \times 10^{11}$ molecules cm^{-3}; (□) P = 122 Torr, $[HNO_3] \simeq 5 \times 10^{14}$ molecules cm^{-3}, $[OH]_0 \simeq 1 \times 10^{11}$ molecules cm^{-3}.

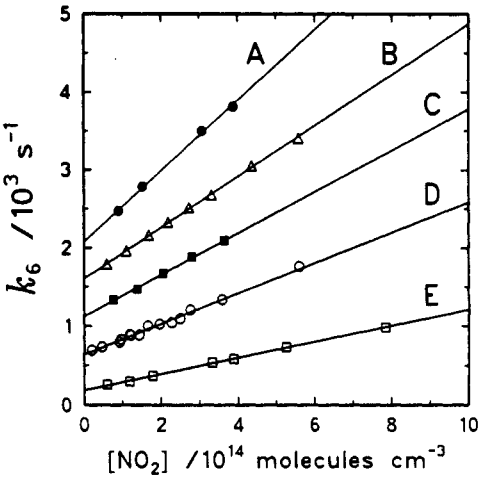

Figure 5. First-order rate coefficient of OH loss (other than reaction 1f), k_6, as a function of NO_2 concentration at 298 K. (A) P = 202 Torr, (B) P = 140 Torr, (C) P = 104 Torr, (D) P = 63 Torr, (E) P = 26 Torr. $[HNO_3] \simeq 1 \times 10^{15}$ molecules cm^{-3} except in set B ($[HNO_3] = 0$ and $[H_2O_2] \simeq 5 \times 10^{13}$ molecules cm^{-3}); $[OH]_0 \simeq (1-2) \times 10^{11}$ molecules cm^{-3}. The lines were shifted upward by 2000, 1500, 1000, and 500 s^{-1}, respectively, for lines A–D.

A linear least-squares fitting of k_5 to eq 21 gave $k_3 = (7.29 \pm 0.26) \times 10^{-13}$ cm^3 molecule^{-1} s^{-1} and $k'' = 12 \pm 87$ s^{-1}. The estimated systematic errors, ±18%, are slightly greater because the fitting of the OH temporal profile is less accurate due to greater values of k_6. Therefore, $k_3 = (7.3 \pm 1.8) \times 10^{-13}$ cm^3 molecule^{-1} s^{-1} is reported, with the uncertainties representing 95% confidence limits.

Reaction 15 (when H_2O_2 was present) and 20 (when HNO_3 was present) did not interfere with the measurement of k_3 because reaction 1f was much more rapid than reactions 15 and 20 when $[CS_2] = 4.8 \times 10^{16}$ molecules cm^{-3} and $k_{1f} \simeq (1.8-2.2) \times 10^{-13}$ cm^3 molecule^{-1} s^{-1}. This is also consistent with our k_5 values which are independent of the OH sources.

The k_3 value determined in this work agrees with that reported by Lovejoy et al.,[18] $(9.1 \pm 3.5) \times 10^{-13}$ cm^3 molecule^{-1} s^{-1} at 299 K. Because the concentrations of NO employed in our study, $(0.7-9.2) \times 10^{15}$ molecules cm^{-3}, cover a much greater range than those by Lovejoy et al., $(0.2-1.0) \times 10^{15}$ molecules cm^{-3}, one would normally expect greater accuracy for our determination of k_3. The lack of dependence on pressure for k_3 indicates that reaction 3 is bimolecular.

3. The $CS_2OH + NO_2$ Reaction. It was found that NO_2 was extremely effective in removing CS_2OH; hence minute concentrations of NO_2 in the range $(0.2-3.4) \times 10^{14}$ molecules cm^{-3} were used in order to maintain a suitable OH decay rate. Again, the values of k_6 were initially measured from the $OH + NO_2$ system, and they are relatively greater than those in the study of $CS_2OH + O_2$ reaction. The reaction

$$OH + NO_2 + M \rightarrow HNO_3 + M \qquad (22)$$

in which $k_{22}^0 = (1.2 \pm 0.4) \times 10^{-30}$ cm^6 molecule^{-2} s^{-1} for M = He,[22] and $k_{22}^\infty = (2.4 \pm 1.2) \times 10^{-11}$ cm^3 molecule^{-1} s^{-1} at 300 K,[21] contributes dominantly to k_6. Plots of k_6 versus $[NO_2]$ are shown in Figure 5 for $26 \le P/\text{Torr} \le 202$. The bimolecular rate coefficients were determined to be 1.02 ± 0.02, 1.95 ± 0.06, 2.66 ± 0.08, 3.27 ± 0.03, and 4.53 ± 0.12 (all in units of 10^{-12} cm^3 molecule^{-1} s^{-1}) for P = 26, 63, 104, 140, and 202 Torr, respectively, in agreement with previous measurements.[22]

Table III lists the experimental conditions and the results for the study of the reaction $CS_2OH + NO_2$. A plot of k_5 versus $[NO_2]$ at 298 K and P = 26–202 Torr is illustrated in Figure 6.

(22) The listed coefficient is the average value of five reports: (a) Westenberg, A. A.; deHaas, N. *J. Chem. Phys.* **1972**, *57*, 5375. (b) Anastasi, C.; Smith, I. W. M. *J. Chem. Soc., Faraday Trans. 2* **1976**, *72*, 1459. (c) Erler, K.; Zellner, R.; Smith, I. W. M. *Ber. Bunsen-Ges. Phys. Chem.* **1977**, *81*, 22. (d) Reference 20c. (e) Reference 20d.

TABLE III: Summary of Experimental Conditions, Decay Parameters of the [OH] Temporal Profile, and the Rate Coefficients for the Study of the Reaction $CS_2OH + NO_2 \rightarrow$ Products in Helium at 298 K[a]

expt no.	P/Torr	$[CS_2]/10^{16}$ [b]	$[NO_2]/10^{14}$ [b]	$\alpha/10^4$ s^{-1}	$\beta/10^7$ s^{-2}	$\gamma/10^4$ s^{-1}	$k_6/10^2$ s^{-1}	$k_5/10^3$ s^{-1}
1	26	4.52	0.84	1.95 ± 0.19	2.28 ± 0.25	1.46 ± 0.16	2.76 ± 0.06	3.84 ± 2.25
2	60	4.89	2.78	7.05 ± 0.76	22.61 ± 2.57	5.38 ± 0.63	4.55 ± 0.21	12.41 ± 7.74
3		4.89	1.18	3.98 ± 0.39	7.09 ± 0.74	2.61 ± 0.29	3.34 ± 0.18	4.65 ± 1.80
4		4.89	1.09	3.52 ± 0.25	5.81 ± 0.46	2.40 ± 0.20	2.89 ± 0.12	4.72 ± 1.49
5		4.82	2.22	3.67 ± 0.38	11.02 ± 1.27	2.59 ± 0.32	4.85 ± 0.31	9.45 ± 4.73
6	63	4.71	1.00	3.01 ± 0.14	5.13 ± 0.27	2.08 ± 0.12	3.02 ± 0.07	4.98 ± 1.12
7		4.71	0.545	2.95 ± 0.11	3.08 ± 0.13	1.84 ± 0.08	2.07 ± 0.04	2.46 ± 0.37
8		4.71	1.47	3.60 ± 0.16	8.23 ± 0.41	2.49 ± 0.13	4.13 ± 0.19	6.72 ± 1.42
9		4.89	1.30	3.78 ± 0.15	7.95 ± 0.34	2.56 ± 0.12	3.85 ± 0.12	5.91 ± 1.06
10		4.90	0.481	3.49 ± 0.15	3.39 ± 0.16	2.32 ± 0.11	2.03 ± 0.07	2.54 ± 0.48
11		4.93	2.59	3.69 ± 0.25	13.31 ± 1.05	2.54 ± 0.22	6.30 ± 0.19	10.71 ± 3.47
12		4.96	1.06	3.44 ± 0.16	6.73 ± 0.35	2.29 ± 0.12	3.40 ± 0.10	5.33 ± 1.08
13		5.02	2.12	3.65 ± 0.25	11.69 ± 0.94	2.44 ± 0.21	5.41 ± 0.16	8.99 ± 2.77
14		5.06	2.94	4.15 ± 0.30	17.94 ± 1.56	2.92 ± 0.28	7.14 ± 0.21	13.23 ± 4.65
15		5.09	0.240	3.17 ± 0.09	1.75 ± 0.06	2.06 ± 0.07	2.11 ± 0.06	1.21 ± 0.16
16		5.14	1.77	3.47 ± 0.15	9.50 ± 0.46	2.31 ± 0.12	4.92 ± 0.15	7.52 ± 1.46
17		5.20	2.37	3.41 ± 0.16	11.64 ± 0.65	2.33 ± 0.14	6.06 ± 0.18	9.87 ± 2.26
18	104	5.40	1.63	5.54 ± 0.30	14.45 ± 0.85	3.53 ± 0.22	2.85 ± 0.22	6.78 ± 1.41
19	140	5.58	2.32	5.61 ± 0.28	20.09 ± 1.12	3.79 ± 0.22	8.56 ± 0.26	9.72 ± 2.21
20		5.56	1.16	4.81 ± 0.27	9.72 ± 0.59	3.16 ± 0.20	4.88 ± 0.15	5.11 ± 1.18
21		5.52	3.44	5.23 ± 0.34	26.98 ± 2.01	3.54 ± 0.30	12.29 ± 0.37	14.45 ± 4.22
22		5.49	0.55	5.58 ± 0.39	6.83 ± 0.51	3.80 ± 0.29	2.92 ± 0.09	3.27 ± 0.98
23		5.45	2.82	5.34 ± 0.35	23.80 ± 1.81	3.57 ± 0.30	10.28 ± 0.31	12.11 ± 3.61
24		5.43	1.70	6.57 ± 0.35	20.00 ± 1.14	4.49 ± 0.27	6.64 ± 0.20	8.45 ± 1.02
25	202	4.94	3.08	8.53 ± 0.66	52.59 ± 4.72	5.34 ± 0.52	17.02 ± 0.07	14.39 ± 4.40

[a] The uncertainties represent 1 standard deviation. [b] In units of molecules cm^{-3}.

TABLE IV: Summary of Experimental Conditions and Rate Coefficients for the Reactions of CS_2OH

reaction	$k/10^{-14}$ cm^3 molecule^{-1} s^{-1}	T/K	P/Torr	[reactant]/10^{15} molecules cm^{-3}	method[a]	investigator
$CS_2OH + O_2$	3.1 ± 0.6	298	65–140	16–325	LP LIF/TP	this work
	2.9 ± 1.1	251–348	680 ± 20	45–22200	LP LIF/SS	Hynes et al.[13]
	2.6 ± 1.0	249–299	50	<260	LP LIF/TP	Murrells et al.[14]
$CS_2OH + NO$	73 ± 18	298	64–122	0.7–9.2	LP LIF/TP	this work
	91 ± 35	299	50	0.2–1.4	LP LIF/TP	Lovejoy et al.[18]
	130 ± 40	249	50	0.2–1.0	LP LIF/TP	Lovejoy et al.[18]
$CS_2OH + NO_2$	4200 ± 1000	298	26–202	0.02–0.34	LP LIF/TP	this work
$CS_2OH + O_3$	90 ± 30	298	150	0.2–1.0	LP LIF/SS	Bulatov et al.[16]

[a] LP LIF, laser photolysis with laser-induced fluorescence detection; SS, steady-state analysis; TP, temporal-profile analysis.

Again, data from different sources of OH and total pressures showed no observable differences. With k_5 expressed as

$$k_5 = k_7[NO_2] + k''' \qquad (23)$$

a linear least-squares fitting of k_5 to eq 23 yielded $k_7 = (4.20 \pm 0.10) \times 10^{-11}$ cm^3 molecule^{-1} s^{-1} and $k''' = 350 \pm 140$ s^{-1}.

Photolysis of NO_2 in the UV region generates O atoms which may react rapidly with CS_2OH. However, the small absorption cross section of NO_2 at 248 nm, $\sim 2.8 \times 10^{-20}$ cm^2 molecule^{-1},[21] and the small concentration of NO_2 ($< 3.4 \times 10^{14}$ molecules cm^{-3}) employed in these experiments resulted in an estimated production of O atoms less than 2×10^{11} molecules cm^{-3}, too small to have any effect on the measurements of k_7. The agreement between the effective bimolecular rate coefficients for reaction 22 determined in this study and those reported earlier also indicates that the reactions involving O atoms were probably unimportant in the study, even though the rate coefficient of the reaction

$$O + OH \rightarrow O_2 + H \qquad (24)$$

in which $k_{24} = 3.3 \times 10^{-11}$ cm^3 molecule^{-1} s^{-1} is relatively large.[20] Taking the estimated ±18% systematic errors into account, we report $k_7 = (4.2 \pm 1.0) \times 10^{-11}$ cm^3 molecule^{-1} s^{-1}, with the uncertainties representing 95% confidence limits. The lack of dependence on pressure for k_7 indicates that reaction 7 is bimolecular; the products are yet to be determined.

The experimental measurements of rate coefficients for the reactions of CS_2OH are summarized in Table IV. To our knowledge, no study on reaction 7 other than this work has been reported. The rate coefficient k_7 is approximately 1400 times greater than k_2 ($CS_2OH + O_2$), and 60 times greater than k_3 (CS_2OH+NO). However, reaction 7 contributes <1% of the rate enhancement of OH + CS_2 in the atmosphere because most CS_2 is oxidized within the atmospheric boundary layer in which $[NO_2] < 2 \times 10^{13}$ molecules cm^{-3}.[23]

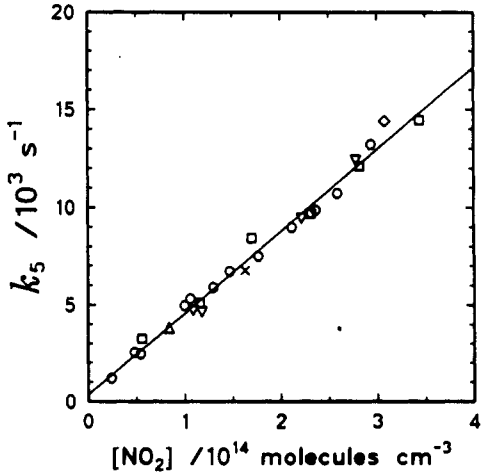

Figure 6. First-order rate coefficient of CS_2OH loss (other than reaction 1r), k_5, as a function of NO_2 concentration at 298 K. $[HNO_3] \simeq 1 \times 10^{15}$ molecules cm^{-3} and $[OH]_0 \simeq (1-2) \times 10^{11}$ molecules cm^{-3} unless noted. (△) $P = 26$ Torr; (▽) $P = 60$ Torr; (○) $P = 63$ Torr; $[HNO_3] \simeq (0.4-2) \times 10^{15}$ molecules cm^{-3}; $[OH]_0 \simeq (1-5) \times 10^{11}$ molecules cm^{-3}; (×) $P = 104$ Torr; (□) $P = 140$ Torr, $[H_2O_2] \simeq 5 \times 10^{13}$ molecules cm^{-3}, $[HNO_3] = 0$; (◇) $P = 202$ Torr.

Our measurements of k_7 provide a rationale for the results reported previously for the study of reaction 1 by Leu and Smith using the discharge-flow/resonance-fluorescence technique.[7] In their work, OH was generated by reacting H with an excess of NO_2. The excess NO_2 removed CS_2OH (hence OH) quite efficiently due to the large reaction rate coefficient k_7. If a reaction mechanism consisting of reactions 1f, 1r, and 7 is used in the steady-state approximation of CS_2OH, the observed effective rate coefficient for OH decay, k'_{obsd}, may be expressed as

$$k'_{obsd} \simeq k_7[NO_2]K_c \quad (25)$$

in which K_c is the equilibrium constant for reaction 1. With $K_c = 8.7 \times 10^{-18}$ cm^3 molecule^{-1} determined previously and $k_7 = 4.2 \times 10^{-11}$ cm^3 molecule^{-1} s^{-1}, an estimated value $[NO_2] \simeq 5 \times 10^{12}$ molecules cm^{-3} employed by Leu and Smith gave $k'_{obsd} \simeq 2 \times 10^{-15}$ cm^3 molecule^{-1} s^{-1}, in agreement with their reported upper limit 3×10^{-15} cm^3 molecule^{-1} s^{-1} at 298 K determined by observing the production rate of OCS. Some heterogeneous reactions of OH on the wall of the flow reactor apparently interfered the determination of the rate coefficient when the loss of OH was following instead; a value 2.9×10^{-14} cm^3 molecule^{-1} s^{-1} was determined.

In the chamber reaction of OH + CS_2 in the presence of O_2 by Barnes et al.,[12] NO_2 was present in both the photolytic and the "dark" experiments. With an estimate of $[NO_2] \simeq 25$ ppm and O_2 at 150 Torr, the effective rate of reaction 7 is ~16% that of k_{obsd} (for reaction 2) under synthetic air at 700 Torr. The contribution from reaction 7 to k_{obsd} would be greater if NO_2 could be somehow cycled back. Although the interference due to reaction 7 may not account for all of the discrepancies between the k_{obsd} values determined by Barnes et al. and those by Jones et al.[10,11] and Hynes et al.,[13] a correction on this effect is expected to reduce the k_{obsd} value reported by Barnes et al. to within the experimental uncertainties of other studies. However, this mechanism still cannot explain the greater k_{obsd} values observed by Becker et al. when H_2O_2 was used as a source of OH.[15] At lower partial pressure of O_2, the interference due to reaction 7 became severe; this may explain why a $[NO_2]$-dependent k_{obsd} was observed at less than 25 Torr of O_2 in the study of reaction 2 by Becker et al.[15]

In summary, the rate coefficients for the reactions of CS_2OH with O_2, NO, and NO_2 have been determined to be $k(CS_2OH+O_2) = (3.1 \pm 0.6) \times 10^{-14}$, $k(CS_2OH+NO) = (7.3 \pm 1.8) \times 10^{-13}$, and $k(CS_2OH+NO_2) = (4.2 \pm 1.0) \times 10^{-11}$ molecule^{-1} s^{-1}. All these reactions appear to be bimolecular and remove CS_2OH efficiently.

Acknowledgment. This research was supported by the National Science Council of the Republic of China.

Registry No. Mercaptooxomethylthio, 123132-54-7; oxygen, 7782-44-7; nitrogen oxide, 10102-43-9; nitrogen dioxide, 10102-44-0.

(23) Finlayson-Pitts, B. J.; Pitts, J. N., Jr. *Atmospheric Chemistry*; Wiley: New York, 1986; p 523.

Unimolecular Decomposition of the Neopentyl Radical

I. R. Slagle, L. Batt,† G. W. Gmurczyk, D. Gutman,*

Department of Chemistry, Catholic University of America, Washington, D.C. 20064

and W. Tsang*

Chemical Kinetics Division, National Institute of Standards and Technology, Gaithersburg, Maryland 20899
(Received: February 5, 1991; In Final Form: April 24, 1991)

The kinetics of the unimolecular decomposition of the neopentyl radical has been investigated. Experimentally, the decomposition was monitored in time-resolved experiments by using a heatable tubular reactor coupled to a photoionization mass spectrometer. The radicals were produced indirectly by pulsed excimer laser photolysis of CCl_4 (to produce CCl_3 + Cl) followed by the rapid reaction between the Cl atoms and neopentane to produce *neo*-C_5H_{11} + HCl. Unimolecular rate constants were determined as a function of bath gas (He, N_2, and Ar), temperature (10 temperatures between 560 and 650 K), and bath gas density ($(3-30) \times 10^{16}$ molecules cm^{-3} (He) and $(6-12) \times 10^{16}$ (N_2, Ar)). The data were fitted within the framework of RRKM theory by using a vibrational model. The high-pressure rate constant in the temperature range studied was determined to be k(neopentyl → isobutene + CH_3) = $10^{13.9\pm0.5}$ exp(−30.9 ± 1.0 kcal mol^{-1}/RT) s^{-1}. The average step sizes down for the bath gases used (adjusted parameters in the RRKM calculations) are comparable: 200 (He), 130 (N_2), and 140 (Ar) cm^{-1} (all ±60 cm^{-1}). The high-pressure-limit rate constant expression for the reverse reaction, nonterminal addition of CH_3 to isobutene, was obtained from thermochemical calculations by using the results of this study: k(CH_3 + isobutene → neopentyl) = 3.7×10^{-13} exp(−10.6 kcal mol^{-1}/RT) cm^3 molecule^{-1} s^{-1}. The Arrhenius parameters of this addition reaction indicate that nonterminal addition is inhibited relative to terminal addition mostly by a larger energy barrier to addition, as opposed to possible entropic effects.

Introduction

The decomposition of alkyl radicals is an important part of the chemical kinetics of many high-temperature processes including the pyrolysis and oxidation of hydrocarbons.[1-3] For example, in hydrocarbon combustion, the competition between the unimolecular decomposition and the oxidation of the alkyl radicals is a key factor in determining many important properties of combustion, such as the nature and importance of products formed, sooting characteristics, and flame speeds. In addition, these decompositions often result in the replacement of the relatively unreactive carbon-centered radical with the more reactive hydrogen atom (e.g., *i*-C_3H_7 → C_3H_6 + H).

Existing experimental determinations of the alkyl-radical decomposition rate constants often show wide scatter.[4] This is due

† Permanent address: Department of Chemistry, University of Aberdeen, Aberdeen, Scotland.

(1) Warnatz, J. In *Combustion Chemistry*; Gardiner, W. C., Jr., Ed.: Springer-Verlag: New York, 1984.
(2) Hucknall, K. J. *Chemistry of Hydrocarbon Combustion*; Chapman and Hall: New York, 1985.
(3) Westbrook, C. K.; Dryer, F. L. *Prog. Energy Combust. Sci.* **1984**, *10*, 1.
(4) Kerr, J. A.; Lloyd, A. C. *Q. Rev. Chem. Soc.* **1968**, *22*, 549.

0022-3654/91/2095-7732$02.50/0